**Cell Reports, Volume *35***

## Supplemental information

# Dysregulation of the mesoprefrontal dopamine circuit mediates an early-life stress-induced synaptic imbalance in the prefrontal cortex

**Won Chan Oh, Gabriela Rodríguez, Douglas Asede, Kanghoon Jung, In-Wook Hwang, Roberto Ogelman, McLean M. Bolton, and Hyung-Bae Kwon**

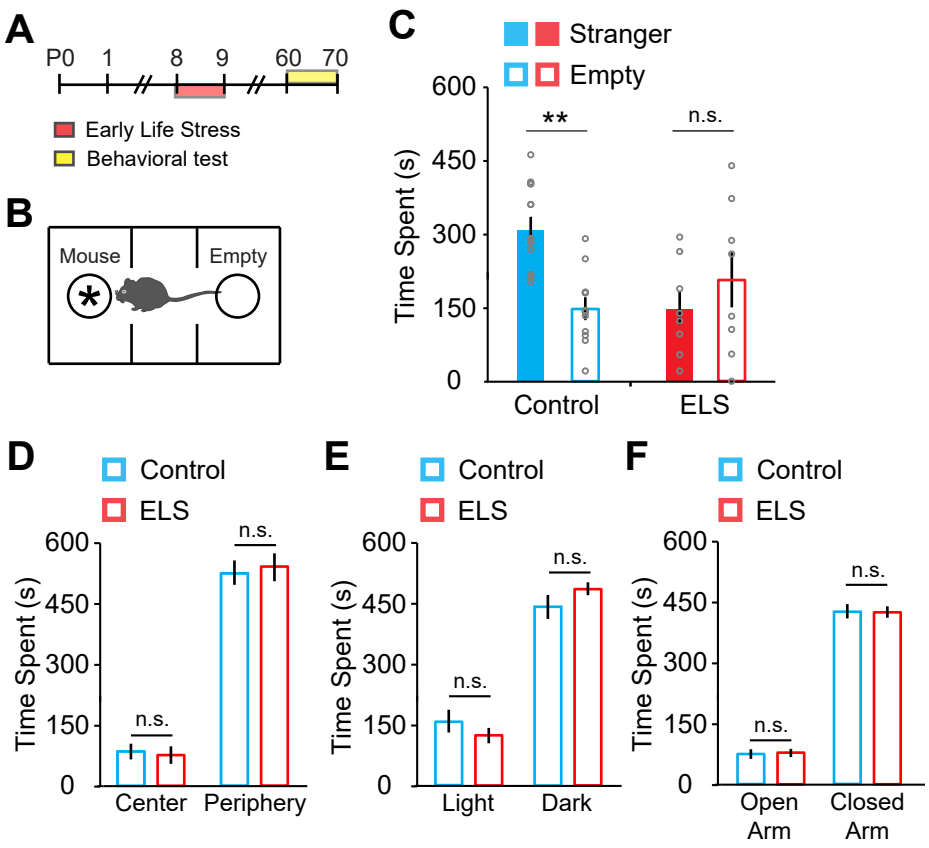


**Fig. S1. ELS adult mice exhibit impaired social behavior with normal levels of anxiety behaviors, Related to Figures 1-4. (A)** Experimental timeline. P, postnatal day. **(B)** Schematic illustrating the three-chamber social preference test. **(C)** Time spent in the chamber of a stranger mouse or the chamber of empty cage during a 10-min test period (control, n=11; ELS, n=8). (**D**) Time spent in the center or periphery of the open field during a 10-min test period (control, n=11; ELS, n=13). (**E**) Time spent in the light or dark zone of the light-dark compartments during a 10-min test period (control, n=11; ELS, n=13). (**F**) Time spent in the open or closed arm zone of the elevated plus-maze during a 10-min test period (control, n=11; ELS, n=13). $^{**}P < 0.01$. Error bars represent s.e.m.; n.s., not significant.

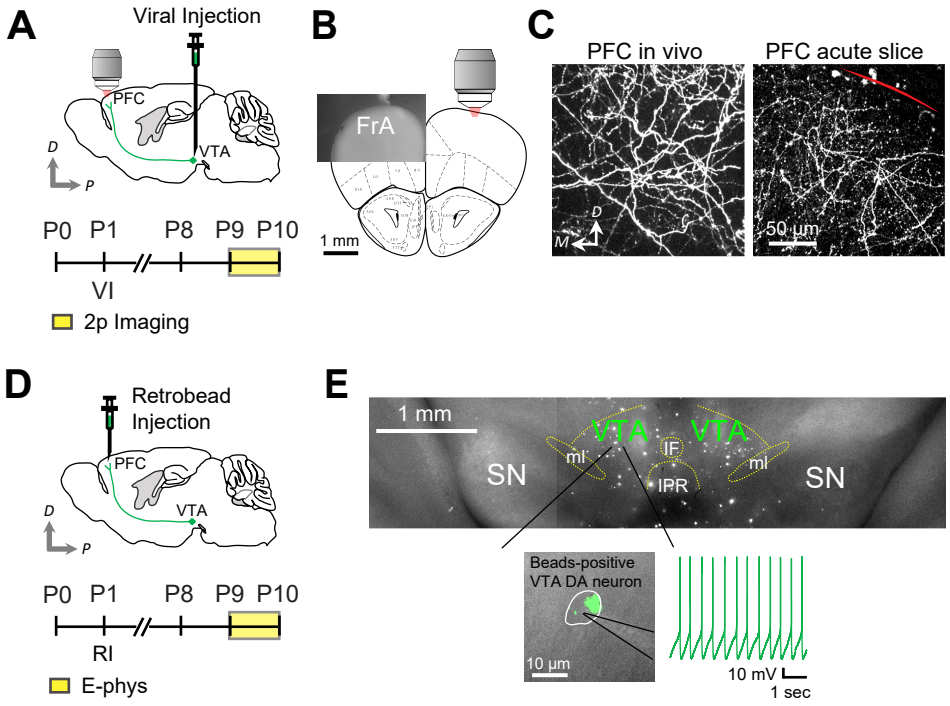


**Fig. S2. VTA DA neurons projecting to DL-PFC are spontaneously active in early postnatal stages, Related to Figure 1 and 2. (A)** Schematic drawing of virus injection for selectively expressing red fluorescent protein (tdTomato) in VTA DA neurons using DAT-Cre mice and *in vivo* imaging site. Experimental timeline. P, postnatal day. **(B)** Diagram of the mouse dorsolateral prefrontal cortex (DL-PFC covering frontal association cortex, FrA) in a coronal section showing *ex vivo* imaging site. **(C)** Widely spread and highly dense axonal arborizations of VTA DA neurons were observed in the developing DL-PFC *in vivo* and in acute cortical brain slices at P9. **(D)** Schematic depiction of retrograde beads injection into DL-PFC and experimental timeline. **(E)** An overlay of fluorescent and DIC images of an acute midbrain slice containing the VTA at P9 (top). A retrogradely labeled (green beads) putative VTA DA neuron (bottom) exhibits spontaneous action potential spikes recorded by whole-cell current clamp mode.

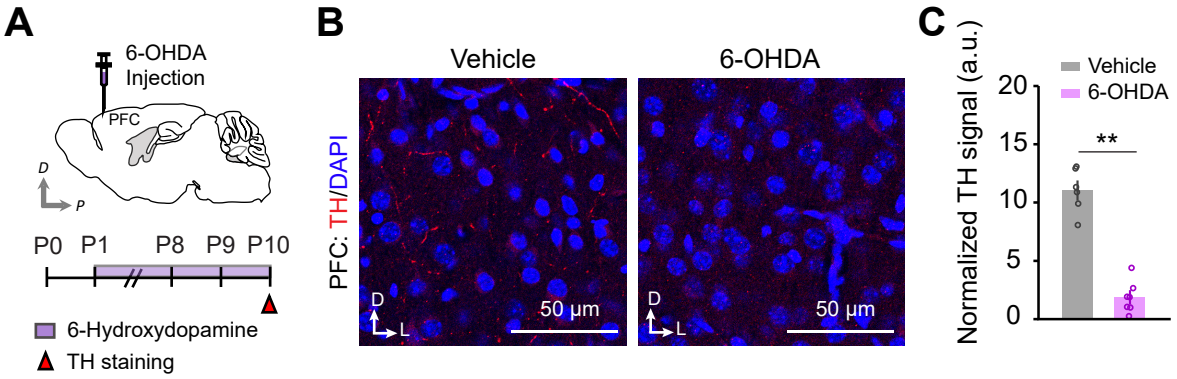


**Fig. S3. 6-OHDA-induced denervation of dopaminergic terminals in PFC, Related to Figure 4.** **(A)** Schematic of 6-OHDA injection into PFC and experiment timeline. **(B)** Confocal images of dopaminergic axons stained with tyrosine hydroxylase (TH) in vehicle (Left)- or 6-OHDA (Right)-injected mice at P10 and **(C)** quantifications of TH fluorescent signals (vehicle-injected mice, n=6; 6-OHDA-injected mice, n=7). $^{**}P < 0.01$. Error bars represent s.e.m.

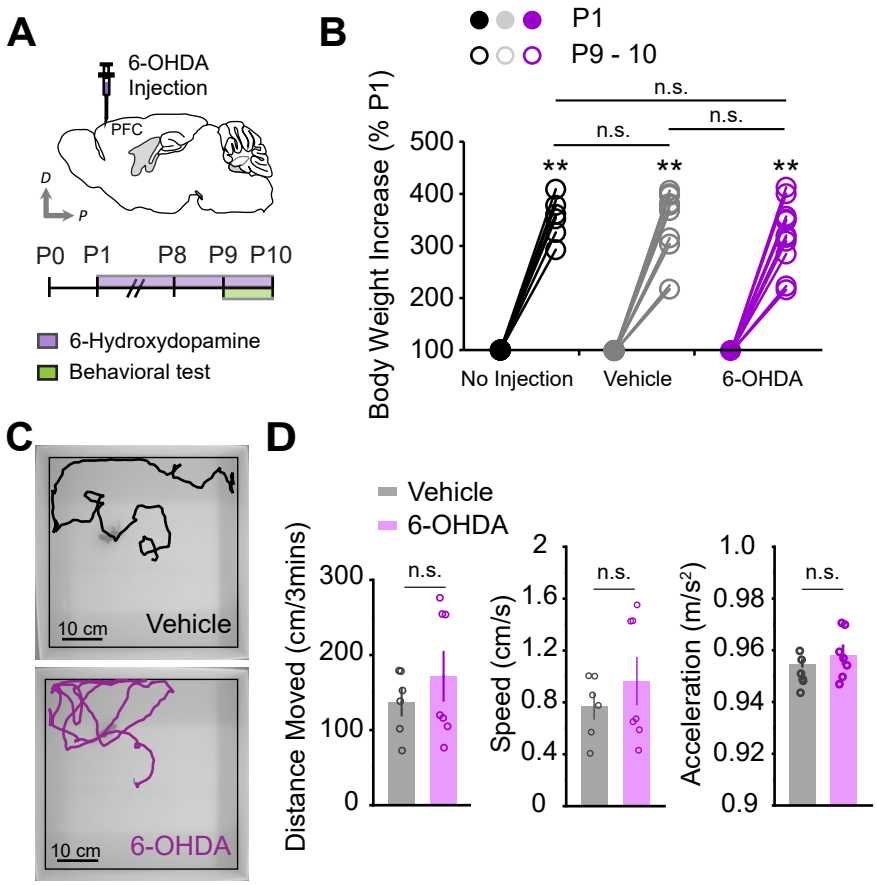


**Fig. S4. The effect of loss of DA axons in DL-PFC on body weights and locomotion, Related to Figure 4. (A)** Schematic of 6-OHDA injection into DL-PFC and experiment timeline. **(B)** Summary graph of body weight changes from no injection, vehicle-, or 6-OHDA-injected mice at P9-10 (no injection, n=9; vehicle, n=10; 6-OHDA, n=11). **(C)** Example movement traces of vehicle (Top)- and 6-OHDA (Bottom)-injected mice at P10. **(D)** Comparison of total distance moved (Left), movement speed (Middle), and movement acceleration (Right) between vehicle- and 6-OHDA-injected mice (vehicle, n=6; 6-OHDA, n=7). $^{**}P < 0.01$. Error bars represent s.e.m.; n.s., not significant.